nature chemistry

Article

https://doi.org/10.1038/s41557-023-01384-x

Organocatalytic aromatization-promoted umpolung reaction of imines

Received: 7 November 2022

Accepted: 24 October 2023

Published online: 7 December 2023

Check for updates

Ye-Hui Chen[1,3], Meng Duan[2,3], Si-Li Lin[1], Yu-Wei Liu[1], Jun Kee Cheng[1], Shao-Hua Xiang[1], Peiyuan Yu[1], Kendall N. Houk[2] ✉ & Bin Tan[1] ✉

The umpolung functionalization of imines bears vast synthetic potential, but polarity inversion is less efficient compared with the carbonyl counterparts. Strong nucleophiles are often required to react with the N-electrophiles without catalytic and stereochemical control. Here we show an effective strategy to realize umpolung of imines promoted by organocatalytic aromatization. The attachment of strongly electron-withdrawing groups to imines could enhance the umpolung reactivity by both electronegativity and aromatic character, enabling the direct amination of (hetero)arenes with good efficiencies and stereoselectivities. Additionally, the application of chiral Brønsted acid catalyst furnishes (hetero)aryl C–N atropisomers or enantioenriched aliphatic amines via dearomative amination from N-electrophilic aromatic precursors. Control experiments and density functional theory calculations suggest an ionic mechanism for the umpolung reaction of imines. This disconnection expands the options to forge C–N bonds stereoselectively on (hetero)arenes, which represents an important synthetic pursuit, especially in medicinal chemistry.

Umpolung refers to the reversal of the intrinsic polarity of functional groups, the underlying reactivity principle of many useful chemical reactions otherwise inhibited by the mismatch of electronics[1–6]. Electron-deficient carbonyl groups constitute the most illustrative examples of reactivity umpolung that, under the auspices of N-heterocyclic carbene (NHC) catalysis, enable many important C–C bond formation reactions[7–13]. As a closely related class of functionality, imines are engaged in wide array of transformations that proceed through nucleophilic addition to the electrophilic carbon[14–16]. Synthetic efforts to reverse the usual imine reactivity have, however, not enjoyed the same level of success[17–23]. The weaker electrophilicity of imine carbons could obstruct complete polarity inversion, which often reflects as imperfect site selectivity. An inspirational advance was introduced by Deng and co-workers[18], who designed chiral phase-transfer catalysts to promote generation and reaction of 2-azaallyl anions with enals with high efficiency and selectivities, charting new pathway to chiral amines.

By comparison, Kagan and Fiaud characterized the reactivity umpolung of imine nitrogen on electron-poor α-imine esters almost half a century ago[24]. Successful exploration of this reactivity concept was later achieved by Shimizu[25] mainly for N-alkylation, and Kürti[26] in the synthesis of diaryl-, arylalkyl- and dialkylamines. The reversed electronic profile also renders the N-electrophilic imines to be well-suited precursors of α-amino acid derivatives and amines[27]. Although these schemes do not require transition metal catalysts, effective C-nucleophiles for this chemistry are largely confined to moisture- and air-sensitive organometallic reagents. Moreover, chemoselective N-functionalization was reinforced by the restricted access to C-site due to bulky substituents (Fig. 1a), and the stereochemical control of this stoichiometric process remains elusive. These restrictions provide a strong incentive to develop a catalytic nitrogen umpolung strategy, which could operate for an expanded range of nucleophiles with rigorous control of chemo- and stereoselectivity. The establishment of scuh an approach would signify a major conceptual advance with practical consequences.

[1]Shenzhen Grubbs Institute, Department of Chemistry, Southern University of Science and Technology, Shenzhen, China. [2]Department of Chemistry and Biochemistry, University of California, Los Angeles, CA, USA. [3]These authors contributed equally: Ye-Hui Chen, Meng Duan. ✉e-mail: houk@chem.ucla.edu; tanb@sustech.edu.cn

https://doi.org/10.1038/s41557-023-01384-x

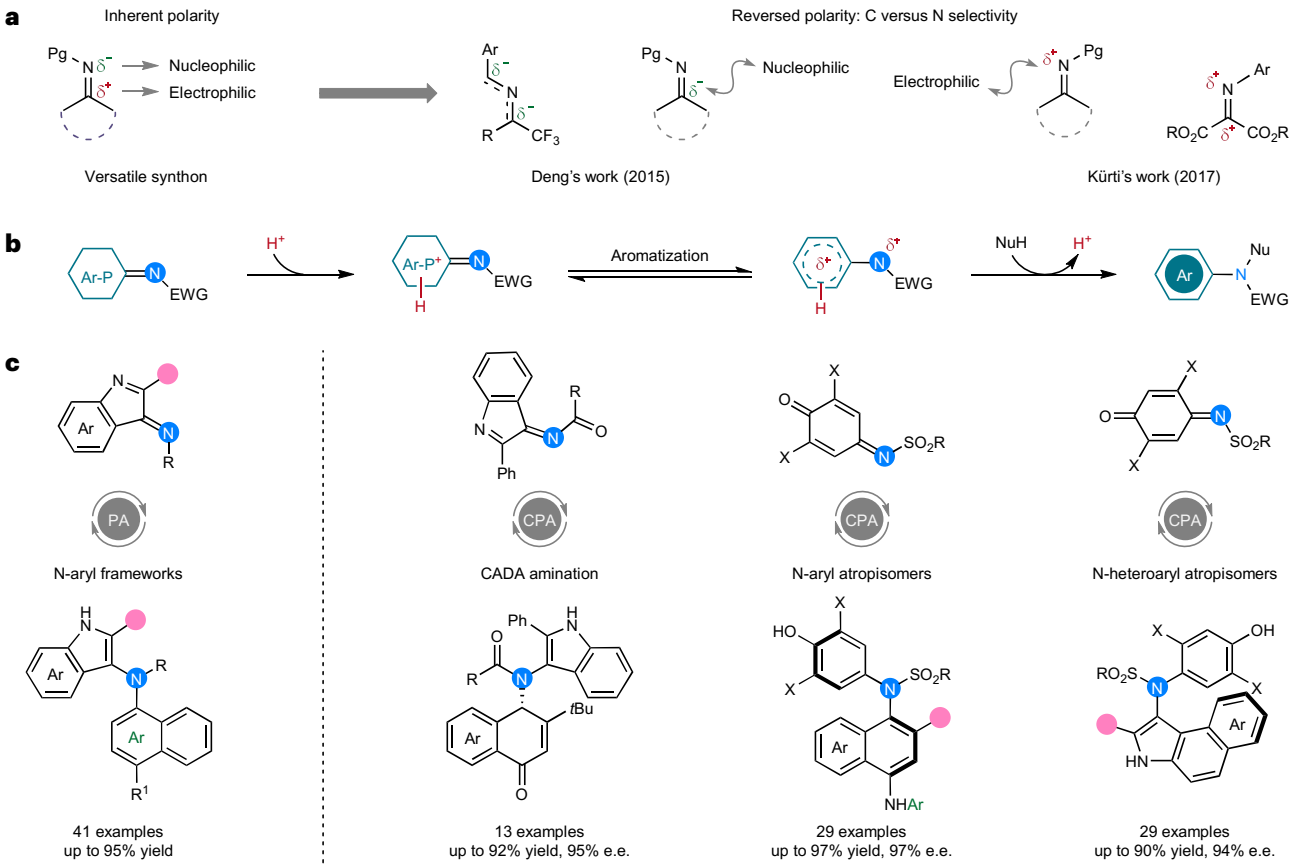

Fig. 1 | Motivation and design for umpolung of imines. a, Inherent polarity of imines and developed strategies for imine umpolung. **b**, Our design for polarity reversal of imine promoted by aromatization. Features: organocatalysis, absolute chemoselectivity control at N atom, mild conditions and versatile asymmetric synthetic applications; EWG, electron-withdrawing group. Ar-P, precursor of aromatic ring. **c**, This work: imine N-functionalization streamlines the syntheses of N-aryl frameworks, aliphatic amines and N-(hetero)aryl atropisomers from indole-derived imines and iminoquinones.

By virtue of the tremendous thermodynamic driving force, an aromatization event could empower challenging transformations that involve C–C bond activation, which are unattainable by conventional approaches[28–31]. The enabling nature of this process led us to surmise that the favourable thermodynamics of aromatization could best tackle the reactivity challenge to achieve umpolung of imines (Fig. 1b). We considered initiating the reaction through protonation of the Lewis basic heteroatom on arene precursors with Brønsted acid catalyst. The delocalization of the developed positive charge to imine nitrogen by resonance is then enhanced by aromatization. This would augment the electrophilicity of imine nitrogen in readiness for nucleophilic addition. The catalytic turnover is accomplished with the release of proton upon formation of the C–N axis.

Of further importance, the strong aromatization-derived driving force should enable extension of the umpolung reactivity to softer nucleophiles such as (hetero)arenes. This would strategically complement the existing suite of transition metal-catalysed C–N cross-coupling[32–37] reactions to assemble aromatic amines, which are ubiquitous substructures in biologically active natural products and drugs[38,39]. As more powerful chiral Brønsted acids[40,41] are being developed to tackle increasingly challenging synthetic problems, we also looked towards applying this catalytic tool to set the configuration of the N-aryl axis. To this end, it is envisioned that bifunctional chiral phosphoric acid (CPA)[42,43] catalysts will be well positioned to effect the proton transfer and activate the reactants. Nonetheless, this polarity inversion strategy comes with the challenging tasks of identifying suitable aromatic precursors and achieving regioselective localization of positive charge on these reactants.

In this Article, we describe how these challenges are successfully addressed in our endeavours to realize the envisioned strategy. As detailed below, imines found on indole and iminoquinones have been developed as effective N-electrophilic heteroarene and arene precursors (Fig. 1c). A variety of aromatic and heteroaromatic nucleophiles could undergo this umpolung reaction, which yield chiral amine frameworks via arene amination or dearomative amination with exquisite stereoselectivity and absolute N-selectivity. The N-arylation of indole-derived imines by 1-naphthols and 1-naphthylamines operated with excellent efficiency in the presence of phosphoric acid to yield 4-aminonaphthalen-1-ols and naphthalene-1,4-diamines that could harbour diverse substituents. The chiral acid catalyst directed the C–N coupling stereoselectively with dearomatization of naphthol nucleophiles, furnishing tertiary amines with attaching indole and naphthalen-1(4*H*)-one moieties. Additionally, the C–N linkage between iminoquinones and naphthylamines or benzoindoles was established with well-defined axial configuration to generate N-(hetero)aryl atropisomers. These catalytic asymmetric dearomatization (CADA) reactions represent an efficient method to rapidly build up molecular three-dimensionality from flat aromatic systems with stereoselectivity upon C–N bond formation[44]. As well as contributing an appealing addition to this toolbox, this chemistry reveals new disconnection for the retrosynthesis of (hetero)aromatic and aliphatic amines in general.

Reaction optimization

The initial phase of the study was aimed at designing imines based on indole as potential heteroaromatic precursors. As a compelling proof of concept, we were encouraged to observe the umpolung reactivity of imine

https://doi.org/10.1038/s41557-023-01384-x

Table 1 | Organocatalytic umpolung of imines to construct *N*-aryl frameworks[a]

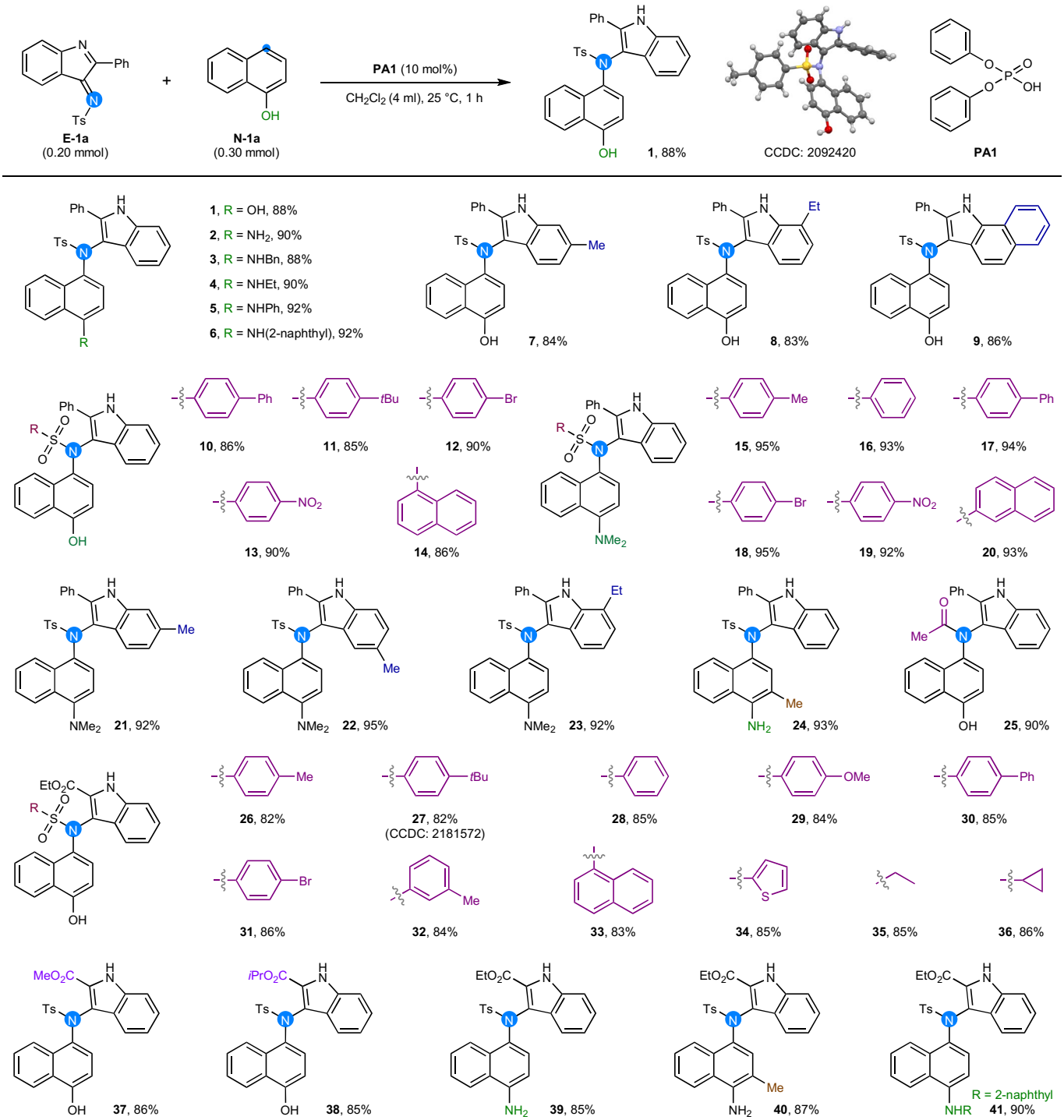

[a]Reaction conditions: phosphoric acid **PA1** (10 mol%), **E-1** or **E-2** (0.20 mmol) and **N-1** or **N-2** (0.30 mmol) were dissolved in CH_2Cl_2 (0.05 M, 4 ml). The mixture was stirred at 25 °C for 0.5–1 h. Isolated yield provided based on imine. Ts, *p*-toluenesulfonyl.

E-1a derived from 2-phenylindole, which bears an electron-withdrawing *N*-tosyl imine group at C3 position. In the presence of phosphoric acid (Table 1), the reaction of **E-1a** with 1-naphthol **N-1a** forged the C–N axis in product **1** in 88% yield under the optimal conditions. Having confirmed the structure of **1** by X-ray diffraction analysis, the substrate generality of this catalytic umpolung reaction was investigated.

Aside from 1-naphthol **N-1a**, 1-naphthylamines were identified as suitable nucleophiles. The free 1-naphthylamine (**2**) and different N-substituted derivatives (**3**–**6**) reacted with N-electrophilic **E-1a** in excellent yields (88–92%). The 2-phenylindoles equipped with 6-methyl or 7-ethyl substituent and benzoindole with additional fused ring afforded the *N*-aryl adducts **7**–**9** in 83–86% yield. On the other hand, the umpolung reaction of 1-naphthol **N-1a** and 2-phenylindoles bearing various arylsulfonyl imines proceeded in good efficiencies (**10**–**14**, 85–90%). Besides phenylsulfonyl with 4-phenyl, 4-*tert*-butyl, 4-bromo- or 4-nitro-substitution (**10**–**13**), 1-naphthylsulfonyl group (**14**) could be applied. Expectedly, the

https://doi.org/10.1038/s41557-023-01384-x

Table 2 | CADA of 1-naphthols via umpolung of imines

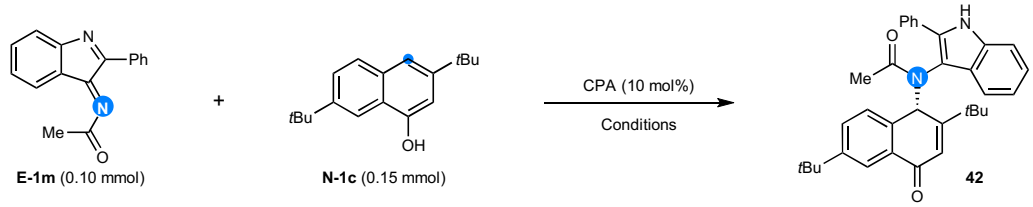

E-1m (0.10 mmol) + **N-1c** (0.15 mmol) → **42**

Reaction development[a]

Entry	CPA	Solvent	Temp.	Time (min)	Yield (%)[b]	e.e. (%)[c]
1	(*R*)-**C1**	CH_2Cl_2	r.t.	5	98	0
2	(*R*)-**C2**	CH_2Cl_2	r.t.	5	97	44
3	(*R*)-**C3**	CH_2Cl_2	r.t.	5	98	18
4	(*R*)-**C4**	CH_2Cl_2	r.t.	5	94	74
5	(*R*)-**C5**	CH_2Cl_2	r.t.	5	98	77
6	(*R*)-**C5**	$CHCl_3$	r.t.	5	96	79
7	(*R*)-**C5**	DCE	r.t.	5	97	82
8	(*R*)-**C5**	toluene	r.t.	5	97	84
9	(*R*)-**C5**	toluene	0 °C	10	97	86
10	(*R*)-**C5**	toluene	–40 °C	20	97 (92)	91

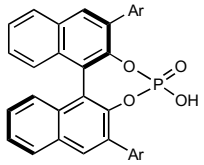

(*R*)-**C1**, Ar = 4-$CF_3C_6H_4$
(*R*)-**C2**, Ar = 9-anthryl
(*R*)-**C3**, Ar = 2,4,6-$Cy_3C_6H_2$
(*R*)-**C4**, Ar = 2,4,6-$Cp_3C_6H_2$
(*R*)-**C5**, Ar = 2,4,6-$iPr_3C_6H_2$

Substrate generality[d]

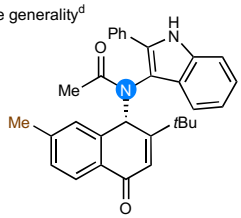

43, 88%, 90% e.e.

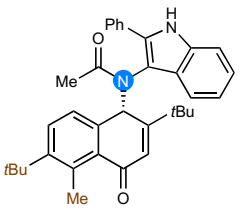

44, 90%, 81% e.e.

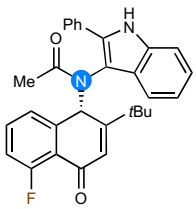

45, 86%, 81% e.e.
CCDC: 2252804

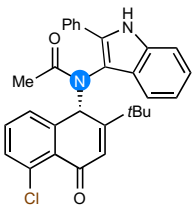

46, 88%, 95% e.e.

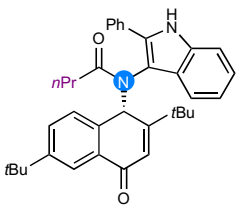

47, 92%, 93% e.e.

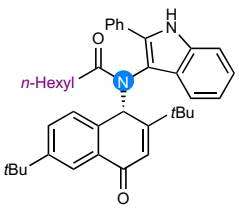

48, 92%, 90% e.e.

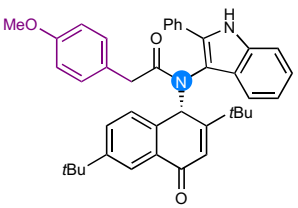

49, 90%, 94% e.e.
CCDC: 2261521

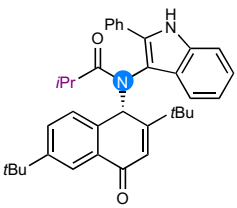

50, 90%, 92% e.e.

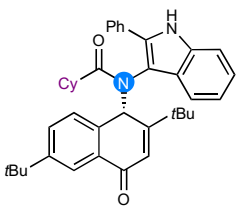

51, 90%, 92% e.e.

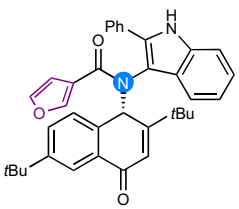

52, 82%, 83% e.e.

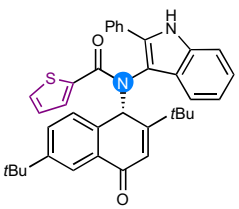

53, 80%, 81% e.e.

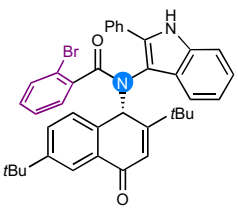

54, 75%, 80% e.e.

[a]Reaction conditions: CPA (10 mol%), **E-1m** (0.10 mmol) and **N-1c** (0.15 mmol) in solvent (4 ml) at the specified temperature. [b]Yields were determined by ^{1}H nuclear magnetic resonance using 1,3,5-trimethoxybenzene as an internal standard. The isolated yield is provided in parentheses based on imine. [c]The e.e. value was determined by chiral stationary HPLC. [d]Reaction conditions: (*R*)-**C5** (10 mol%), **E-1** (0.20 mmol) and **N-1** (0.30 mmol) were stirred at −40 °C for 5 min. Then toluene (4 ml) was added in one portion. The solution was stirred for 20 min at this temperature. The isolated yield is provided based on imine, and the e.e. value was determined by chiral stationary HPLC.

high tolerance to sulfonyl group variations was observed when examined in the context of *N*,*N*-dimethyl-1-naphthylamine (**15**–**20**, 92–95%) while substitution on 2-phenylindole or 1-naphthylamine also had a limited influence on the reaction outcome (**21**–**24**). It was remarkable that the replacement of N-tosyl with the N-acetyl group on imine did not affect the smooth generation of N-aryl amide **25** in 90% yield.

The method could extend beyond 2-phenylindole-based imines: the C2 ester group also efficiently supported the umpolung reactivity of indole-based imines. As with previous cases, sulfonyl connected to phenyl rings of differentiated electronics (**26**–**32**), naphthalene (**33**), thiophene (**34**) and alkyl entities (**35**–**36**) did not impact the amination efficiency with 1-naphthol (82–86%). Other alkyl ester on indole–imines also accommodated the formation of aryl amines **37**–**38** in similar efficiencies. The umpolung reactivity was upheld in this class of imine substrates to afford the amination products **39**–**41** in 85–90% yield when 1-naphthylamine and the derivatives were screened.

https://doi.org/10.1038/s41557-023-01384-x

Table 3 | Catalytic asymmetric umpolung of iminoquinones to synthesize *N*-aryl atropisomers

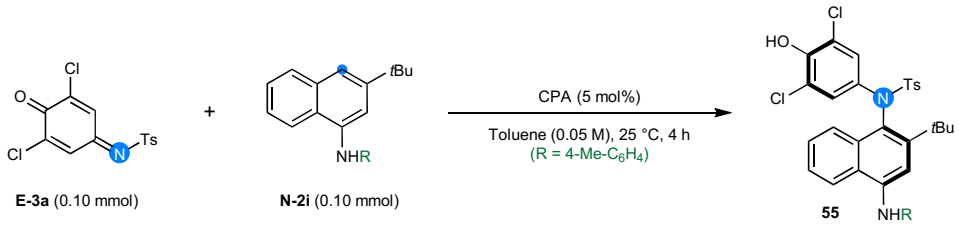

E-3a (0.10 mmol) **N-2i** (0.10 mmol)

Reaction development[a]

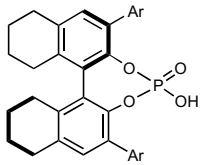

(*R*)-**C6**, Ar = 4-PhC_6H_4
75%, 56% e.e.

(*R*)-**C7**, Ar = 4-$tBuC_6H_4$
87%, 59% e.e.

(*R*)-**C8**, Ar = 4-$CF_3C_6H_4$
82%, 27% e.e.

(*R*)-**C9**, Ar = 3,5-$(CF_3)_2C_6H_3$
85%, 82% e.e.

(*R*)-**C10**, Ar = 1-naphthyl
94%, 90% e.e.

(*R*)-**C11**, Ar = 9-phenanthrenyl
93%, 84% e.e.

(*R*)-**C10**, Ar = 1-naphthyl
95%, 92% e.e. (7.5 mol%)[b]

(*R*)-**C10**, Ar = 1-naphthyl
97%, 94% e.e. (7.5 mol%)[c]

Substrate generality[d]

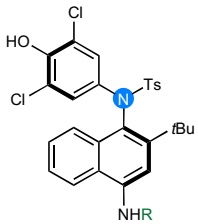

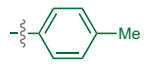

55, 97%, 94% e.e.

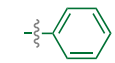

56, 92%, 88% e.e.

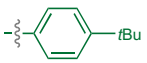

57, 92%, 92% e.e.

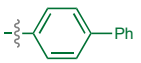

58, 91%, 94% e.e.

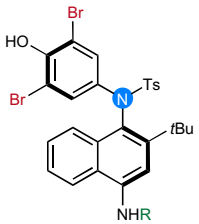

63, 89%, 93% e.e.

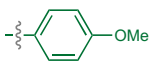

59, 85%, 94% e.e.

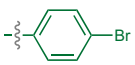

60, 97%, 92% e.e.

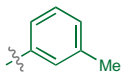

61, 80%, 94% e.e.

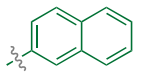

62, 67%, 92% e.e.

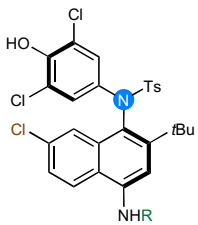

64, 90%, 91% e.e.

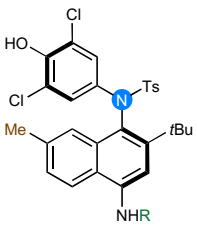

65, 83%, 82% e.e.

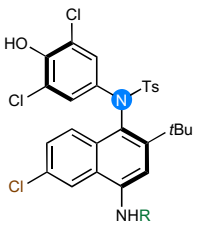

66, 70%, 81% e.e.

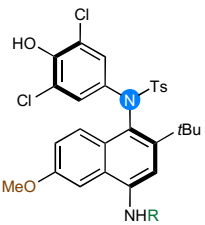

67, 63%, 78% e.e.

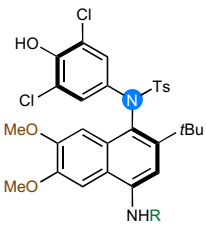

68, 89%, 67% e.e.

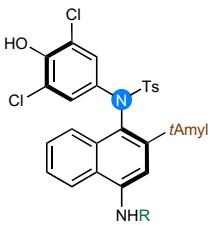

69, 79%, 94% e.e.

R = 4-Me-C_6H_4 for **63-82**

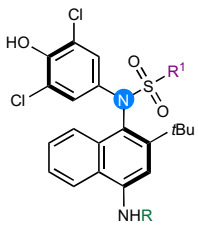

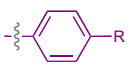

70, R = H, 86%, 95% e.e.
71, R = Br, 86%, 94% e.e.
72, R = CF_3, 92%, 96% e.e.
73, R = NO_2, 88%, 94% e.e.
(CCDC: 2153493)
74, R = OMe, 87%, 93% e.e.
75, R = Ph, 87%, 95% e.e.
76, R = *t*Bu, 88%, 95% e.e.

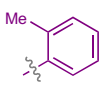

77, 75%, 95% e.e.

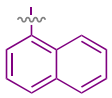

79, 71%, 97% e.e.

81, 88%, 82% e.e.

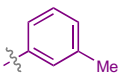

78, 85%, 93% e.e.

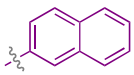

80, 85%, 95% e.e.

82, 93%, 86% e.e.

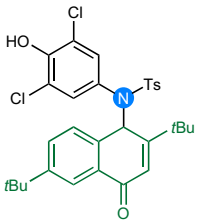

83, 60%, 0% e.e.

[a]Reaction conditions: a solution of CPA (5 mol%), **E-3a** (0.10 mmol) and **N-2i** (0.10 mmol) in toluene (0.05 M, 2 ml) was stirred at 25 °C under N_2 for 4 h, unless noted otherwise. The isolated yield is provided based on imine, and the e.e. value was determined by chiral stationary HPLC. [b]7.5 mol% of catalyst loading. [c]7.5 mol% of catalyst loading and anhydrous toluene. [d]Reaction conditions: a solution of (*R*)-**C10** (7.5 mol%), **E-3** (0.20 mmol) and **N-2** (0.20 mmol) in anhydrous toluene (0.05 M, 4 ml) was stirred at 25 °C under N_2 for about 4 h. The isolated yield is provided based on imine, and the e.e. value was determined by chiral stationary HPLC.

Following this development and our findings on the construction of atropisomeric frameworks, we recognized that the new C–N axis could be set stereoselectively in an adequate substitution environment, hence offering a rapid avenue to aryl C–N atropisomers. Organocatalysis has become a reliable tool to acquire these axially chiral compounds, which encompass anilides[45,46], imides[47], urazoles[48] and quinazolinones[49]. Nonetheless, implementing organocatalytic control for direct formation of chiral C–N bond by atroposelective cross-coupling of sulfonamides with arenes such as naphthols and 1-naphthylamines remains underexplored. As such, developing the asymmetric variant of the outlined C–N cross-coupling protocol would not only expand the utility of this umpolung strategy but also diversify the collection of (hetero)aryl frameworks with a chiral C–N axis[47].

As a starting point to examine this hypothesis, CPA catalyst (*R*)-**C1** was directed to the reaction of 3,7-di-*tert*-butylnaphthalen-1-ol (**N-1c**) with 2-phenylindole-based imine **E-1m**, which bears a C3-*N*-acetyl imine. Intriguingly, this led in high yield to a dearomatized compound **42** instead of an atropisomeric *N*-aryl product in 5 min (Table 2, entry 1). As the aryl side chains at the 3,3′ positions of CPA were varied (entries 2–5), we identified that (*R*)-**C5** with 2,4,6-triisopropyl substituents afforded the best stereoselectivity control (entry 5, 77% enantiomeric excess (e.e.)). Subsequent optimization (entries 6–10) established that the stereoselectivity of this asymmetric dearomative amination improved at lower temperature in toluene, providing **42** in 92% isolated yield with 91% e.e. at −40 °C after 20 min (entry 10).

https://doi.org/10.1038/s41557-023-01384-x

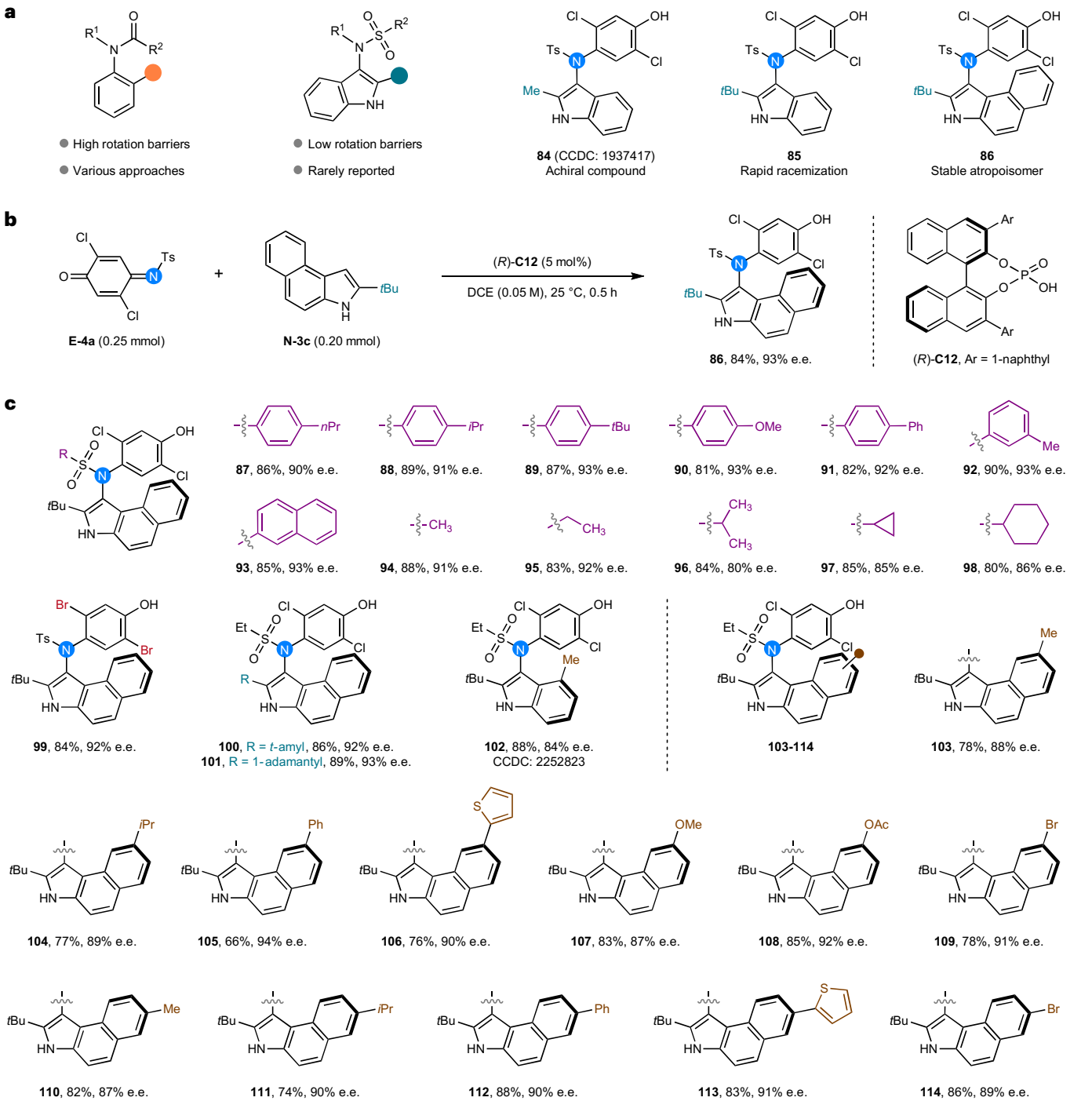

Fig. 2 | The synthesis of atropisomeric N-heteroaryls via catalytic asymmetric umpolung reaction of iminoquinones with C-2 substituted indoles. **a**, Research status of axially chiral N-(hetero)aryl frameworks and initial evaluation of axial stability. **b**, The established optimal conditions for catalytic asymmetric umpolung reaction of iminoquinones with C-2 substituted indoles. **c**, Substrate generality. Reaction scale: 0.25 mmol of **E** and 0.20 mmol of **N**.

The generality of this umpolung transformation was then examined (Table 2). All tested 1-naphthols with alkyl or halogen substituent achieved successful reactions with **E-1m** within 30 min, generating chiral amines **43**–**46** in high yields (86–90%) and commendable enantioselectivities (81–95% e.e.). This chemistry embraced a high tolerance towards differing *N*-acyl components. The reaction yields (90–92%) and stereoselectivities (90–93% e.e.) were unaffected by other alkyl acyl groups (**47**–**51**) other than acetyl group, whereas *N*-arylacyl imines (**52**–**54**) led to inferior product yields (75–82%) and stereoselectivities (80–83% e.e.).

As we sought to also extend this umpolung strategy to arene precursors, the addition of C3-substituted 1-naphthylamine **N-2i** to N-electrophilic iminoquinone **E-3a** was observed to have evolved through an atroposelective manifold to form *N*-naphthylsulfonamide **55** that features a C–N stereogenic axis. This discovery prompted an optimization study where the 3,3′ sidearm of CPA had notable influence on reaction efficiency and atroposelectivity (Table 3, **C6**–**C11**). A refinement of other parameters (Supplementary Table 3) showed that the reaction with increased catalyst loading (7.5 mol%) in anhydrous toluene offered the most optimal outcome (97% and 94% e.e.),

https://doi.org/10.1038/s41557-023-01384-x

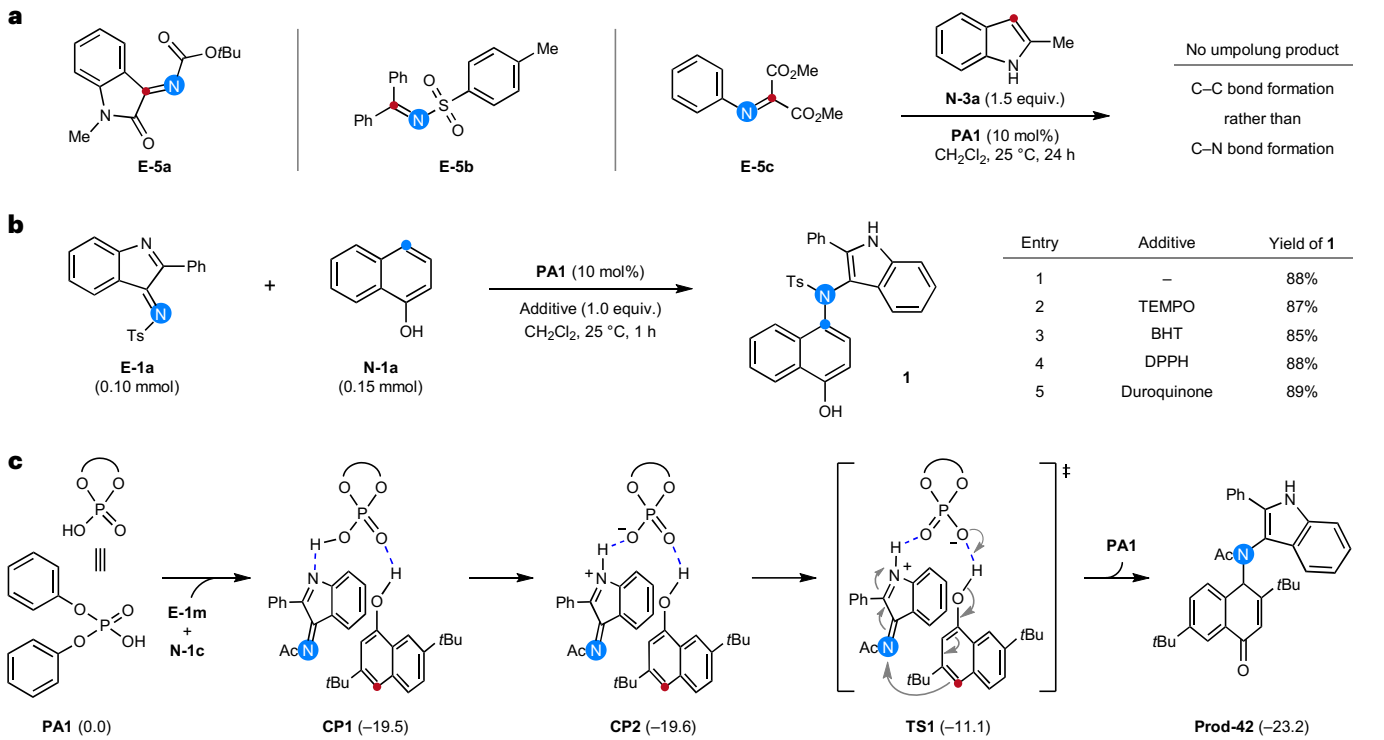

Fig. 3 | Mechanistic investigations. The evaluation of the necessity of the driving force from aromatization and the examination of the possibility of a radical pathway, as well as the proposed reaction pathway for the asymmetric dearomatization process. **a**, Control experiments for imine substrates without driving force from aromatization. Equiv., equivalent. **b**, Radical trapping experiments with conventional radical scavengers. TEMPO, (2,2,6,6-tetramethylpiperidin-1-yl)oxyl; BHT, butylated hydroxytoluene; DPPH, 2,2-diphenyl-1-picrylhydrazyl; duroquinone, 2,3,5,6-tetramethyl-1,4-benzoquinone. **c**, Proposed mechanism for CADA amination based on DFT calculations. Energy differences are given in kcal mol^{-1}.

and these conditions were applied to survey the substrate scope. It was first determined that the modification of amine substituent on 1-naphthylamines (**55**–**62**) did not affect the formation of *N*-aryl axis at C4 position with high atroposelectivities (88–94% e.e.) and in good to excellent yields (67–97%). The compatibility of bromo-substituted iminoquinone (**63**) was also validated. However, the substitution pattern (**64** versus **66** or **67** versus **68**) and electronics (**64** versus **65**), as well as their interplay on the naphthalene core modulated the selectivity control. As an illustration, the e.e. values varied from 91% to 82% and 81% as the 6-Cl (**64**) was replaced by 6-Me (**65**) or 7-Cl group (**66**). A *tert*-amyl group could be installed in place of C3-*tert*-butyl group on the 1-naphthylamine to deliver atropisomerically enriched sulfonamide **69**. The influence of sulfonyl entity on imine was examined next. It could be discerned from products **70**–**80** that the stereocontrol of this umpolung reaction was again not impacted by the decoration pattern and electronic property of the tethered aromatic ring. More substantial variation to the *N*-mesyl (**81**) or *N*-cyclopropyl sulfonyl group (**82**) did not affect the product yields, but enantioselectivities saw slight diminution. It should be noted that dearomatized product **83** was obtained in 60% yield with no enantiopurity when C3-substituted 1-naphthol **N-1c** instead of 1-naphthylamine derivatives was used to react with **E-3a** under standard conditions.

Compared with the benzene derivatives, a constituent five-membered pyrrole would labilize the connecting C–N axis, thereby hampering the chirality control in the related atropisomers (Fig. 2a)[50]. Before initiating the atroposelective synthesis, the potential occurrence of axial chirality in indole sulfonamides **84** and **85** was evaluated with high-performance liquid chromatography (HPLC) analysis on chiral stationary phase, which indicated that compound **84** was achiral while **85** could display atropisomerism. The subsequent asymmetric synthesis attempts nonetheless revealed the low rigidity of this axis, leading to rapid racemization at room temperature in solution (Supplementary Table 5). This issue was adequately addressed by imposing steric encumbrance at the C4 position of indole and the atroposelective preparation of **86** was set to study the umpolung heteroarylation of imines **E-4a** with 1,1′-bi-2-naphthol-derived CPAs as catalysts (Supplementary Table 4). The secured optimal conditions (Fig. 2b) were employed to probe the substrate scope with respect to iminoquinones **E-4** (Fig. 2c). In analogy to previous reactions, the creation of the stereogenic C–N axis occurred in good yields (**86**–**98**, 80–90%) and enantiocontrol (mostly >90% e.e.) for various N-sulfonyl imines. Modest drops of enantiopurities were observed in products with N-isopropyl and N-cycloalkyl sulfonyl imines (**96**–**98**, 80–86% e.e.). The reaction efficiencies and atroposelectivities were generally impervious to substituent modifications on iminoquinone (**99**) and indoles (**100**–**114**). The *tert*-amyl and 1-adamantyl groups sustained the axial rigidity (**100**–**101**). The installation of a methyl group at C4 position was also able to lock the stereogenic axis (**102**). Meanwhile, variegated functionalities such as ester, halogen, heteroaryl and alkyl groups could be introduced on indoles (**103**–**114**). Notably, the formation of these axially chiral heteroaryl sulfonamides was complete within 30 min.

Mechanistic investigations

To clarify the influence of an aromatization event in the developed transformations, imines derived from indolin-2-one (**E-5a**), benzophenone (**E-5b**) and oxomalonate (**E-5c**) were reacted with indole **N-3a** under optimal conditions (Fig. 3a). These substrates did not exhibit any umpolung reactivity and gave C–C bond formation product instead, corroborating that an aromatization process has probably driven the umpolung reaction of imines in this study. To investigate whether this umpolung chemistry develops through a radical manifold, several

radical scavengers were included in the reaction of **E-1a** and **N-1a**. The formation of arylamine **1** in 88% yield was invariably observed in these experiments, thus precluding a radical pathway (Fig. 3b).

To gain further insight into the mechanism of the CADA reaction, density functional theory (DFT) calculations using Gaussian 16 (ref. 51) were performed on the reaction of 2-phenylindole-based imine **E-1m** and 3,7-di-*tert*-butylnaphthalen-1-ol **N-1c** in the presence of biphenyl phosphoric acid (Fig. 3c). Geometry optimizations were conducted by using the ωB97X-D (ref. 52) functional with the 6-31G(d) basis set. Single-point energies and solvent effects in toluene were calculated with the Conductor-like Polarizable Continuum Model [53] at the ωB97X-D/6-311+G(d,p) level of theory. Thermochemistries were corrected with the Head–Gordon and Grimme corrections using GoodVibes version 3.0.1 (ref. 54), with quasiharmonic approximations to entropy[55] and enthalpy[56] and corrected for 233.15 K. Conformation searches were carried out using the conformer–rotamer ensemble sampling tool[57,58] version 2.10.2 with xtb version 6.3.3 (refs. 59–61).

As shown in Fig. 3c, two hydrogen bonds are initially formed between the bifunctional phosphoric acid catalyst and the two substrates **E-1m** and **N-1c** to afford complex **CP1** with a free energy of −19.5 kcal mol^{-1} relative to the separated reactants. Then, the imine substrate is activated by a barrierless proton transfer to form an ion pair intermediate **CP2**. This process enhances the electrophilicity of the imine nitrogen through resonance and delocalization of the positive charge. Subsequently, the dearomative addition of naphthol to the imine nitrogen proceeds via transition state **TS1**, with an activation free energy of 8.5 kcal mol^{-1}. Once the activation barrier is overcome, the dearomatized products are formed along with the release of the free catalyst. Further, CPA (*R*)-**C5** was used to investigate the enantioselectivity origin. Nevertheless, the results from extensive computations with CPA (*R*)-**C5** fail to explain the observed selectivity (Supplementary Fig. 796). Thus, the origins of enantioselectivity presumably involve a more complicated process. This will be the subject of future research.

Conclusions

We have detailed the conception and development of an aromatization-enabled umpolung reaction of imines promoted by a Brønsted acid catalyst. The synergy of the thermodynamic driving force and substrate design, as well as catalyst activation and control, contributed to the high efficiency and chemoselectivity of this imine umpolung strategy. The application of CPA catalysts effectively induces asymmetry in these direct C–N bond formation reactions with indole-based imines and iminoquinones. This approach delivers diverse chiral aliphatic amines via the dearomative amination pathway as well as (N-hetero)aryl frameworks containing stereogenic C–N axis through atroposelective arene C–H amination. This organocatalytic tool enables construction of (axially) chiral amines through an effective umpolung strategy.

Online content

Any methods, additional references, Nature Portfolio reporting summaries, source data, extended data, supplementary information, acknowledgements, peer review information; details of author contributions and competing interests; and statements of data and code availability are available at https://doi.org/10.1038/s41557-023-01384-x.

References

1. Seebach, D. Methods of reactivity umpolung. *Angew. Chem. Int. Ed.* **18**, 239–258 (1979).
2. Smith, A. B. & Adams, C. M. Evolution of dithiane-based strategies for the construction of architecturally complex natural products. *Acc. Chem. Res.* **37**, 365–377 (2004).
3. Shen, B., Makley, D. M. & Johnston, J. N. Umpolung reactivity in amide and peptide synthesis. *Nature* **465**, 1027–1032 (2010).
4. Eymur, S., Göllü, M. & Tanyeli, C. Umpolung strategy: advances in catalytic C–C bond formations. *Turk. J. Chem.* **37**, 586–609 (2013).
5. Zheng, X. et al. Umpolung of hemiaminals: titanocene-catalyzed dehydroxylative radical coupling reactions with activated alkenes. *Angew. Chem. Int. Ed.* **52**, 3494–3498 (2013).
6. Scattolin, T., Deckers, K. & Schoenebeck, F. Efficient synthesis of trifluoromethyl amines through a formal umpolung strategy from the bench-stable precursor $(Me_4N)SCF_3$. *Angew. Chem. Int. Ed.* **56**, 221–224 (2017).
7. Enders, D., Niemeier, O. & Henseler, A. Organocatalysis by N-heterocyclic carbenes. *Chem. Rev.* **107**, 5606–5655 (2007).
8. Bugaut, X. & Glorius, F. Organocatalytic umpolung: N-heterocyclic carbenes and beyond. *Chem. Soc. Rev.* **41**, 3511–3522 (2012).
9. Mahatthananchai, J. & Bode, J. W. On the mechanism of N-heterocyclic carbene-catalyzed reactions involving acyl azoliums. *Acc. Chem. Res.* **47**, 696–707 (2014).
10. Flanigan, D. M., Romanov-Michailidis, F., White, N. A. & Rovis, T. Organocatalytic reactions enabled by N-heterocyclic carbenes. *Chem. Rev.* **115**, 9307–9387 (2015).
11. Nakano, Y. & Lupton, D. W. Enantioselective N-heterocyclic carbene catalysis by the umpolung of α,β-unsaturated ketones. *Angew. Chem. Int. Ed.* **55**, 3135–3139 (2016).
12. Wang, M. H. & Scheidt, K. A. Cooperative catalysis and activation with N-heterocyclic carbenes. *Angew. Chem. Int. Ed.* **55**, 14912–14922 (2016).
13. Guo, C., Fleige, M., Janssen-Müller, D., Daniliuc, C. G. & Glorius, F. Cooperative N-heterocyclic carbene/palladium-catalyzed enantioselective umpolung annulations. *J. Am. Chem. Soc.* **138**, 7840–7843 (2016).
14. Kobayashi, S. & Ishitani, H. Catalytic enantioselective addition to imines. *Chem. Rev.* **99**, 1069–1094 (1999).
15. Kobayashi, S., Mori, Y., Fossey, J. S. & Salter, M. M. Catalytic enantioselective formation of C–C bonds by addition to imines and hydrazones: a ten-year update. *Chem. Rev.* **111**, 2626–2704 (2011).
16. Hummel, J. R., Boerth, J. A. & Ellman, J. A. Transition-metal-catalyzed C–H bond addition to carbonyls, imines, and related polarized π bonds. *Chem. Rev.* **117**, 9163–9227 (2017).
17. Waser, M. & Novacek, J. An organocatalytic biomimetic strategy paves the way for the asymmetric umpolung of imines. *Angew. Chem. Int. Ed.* **54**, 14228–14231 (2015).
18. Wu, Y., Hu, L., Li, Z. & Deng, L. Catalytic asymmetric umpolung reactions of imines. *Nature* **523**, 445–450 (2015).
19. Liu, J., Cao, C.-G., Sun, H.-B., Zhang, X. & Niu, D. Catalytic asymmetric umpolung allylation of imines. *J. Am. Chem. Soc.* **138**, 13103–13106 (2016).
20. Chen, P. et al. Phosphine-catalyzed asymmetric umpolung addition of trifluoromethyl ketimines to Morita–Baylis–Hillman carbonates. *Angew. Chem. Int. Ed.* **55**, 13316–13320 (2016).
21. Hu, L., Wu, Y., Li, Z. & Deng, L. Catalytic asymmetric synthesis of chiral γ-amino ketones via umpolung reactions of imines. *J. Am. Chem. Soc.* **138**, 15817–15820 (2016).
22. Patra, A. et al. *N*-Heterocyclic-carbene-catalyzed umpolung of imines. *Angew. Chem. Int. Ed.* **56**, 2730–2734 (2017).
23. Hu, B. & Deng, L. Catalytic asymmetric synthesis of trifluoromethylated γ-amino acids through the umpolung addition of trifluoromethyl imines to carboxylic acid derivatives. *Angew. Chem. Int. Ed.* **57**, 2233–2237 (2018).
24. Fiaud, J.-C. & Kagan, H. B. Une nouvelle synthese D'α amino-acides. Synthese asymetrique de l'alanine. *Tetrahedron Lett.* **11**, 1813–1816 (1970).
25. Niwa, Y., Takayama, K. & Shimizu, M. Electrophilic amination with iminomalonate. *Tetrahedron Lett.* **42**, 5473–5476 (2001).
26. Kattamuri, P. V. et al. Practical singly and doubly electrophilic aminating agents: a new, more sustainable platform for carbon–nitrogen bond formation. *J. Am. Chem. Soc.* **139**, 11184–11196 (2017).

27. Mizota, I. & Shimizu, M. Umpolung reactions of α-imino esters: useful methods for the preparation of α-amino acid frameworks. *Chem. Rec.* **16**, 688–702 (2016).
28. King, R. B. & Efraty, A. Pentamethylcyclopentadienyl derivatives of transition metals. II. Synthesis of pentamethylcyclopentadienyl metal carbonyls from 5-acetyl-1,2,3,4,5-pentamethylcyclo pentadiene. *J. Am. Chem. Soc.* **94**, 3773–3779 (1972).
29. Schleyer, Pv. R. & Pühlhofer, F. Recommendations for the evaluation of aromatic stabilization energies. *Org. Lett.* **4**, 2873–2876 (2002).
30. Babinski, D. J. et al. Synchronized aromaticity as an enthalpic driving force for the aromatic Cope rearrangement. *J. Am. Chem. Soc.* **134**, 16139–16142 (2012).
31. Xu, Y. et al. Deacylative transformations of ketones via aromatization-promoted C–C bond activation. *Nature* **567**, 373–378 (2019).
32. Cho, S.-H., Kim, J.-Y., Kwak, J. & Chang, S. Recent advances in the transition metal-catalyzed twofold oxidative C–H bond activation strategy for C–C and C–N bond formation. *Chem. Soc. Rev.* **40**, 5068–5083 (2011).
33. Louillat, M.-L. & Patureau, F. W. Oxidative C–H amination reactions. *Chem. Soc. Rev.* **43**, 901–910 (2014).
34. Mailyan, A. K. et al. Cutting-edge and time-honored strategies for stereoselective construction of C–N bonds in total synthesis. *Chem. Rev.* **116**, 4441–4557 (2016).
35. Ruiz-Castillo, P. & Buchwald, S. L. Applications of palladium-catalyzed C–N cross-coupling reactions. *Chem. Rev.* **116**, 12564–12649 (2016).
36. Kainz, Q. M. et al. Asymmetric copper-catalyzed C–N cross-couplings induced by visible light. *Science* **351**, 681–684 (2016).
37. Paudyal, M. P. et al. Dirhodium-catalyzed C–H arene amination using hydroxylamines. *Science* **353**, 1144–1147 (2016).
38. Takahashi, I., Suzuki, Y. & Kitagawa, O. Asymmetric synthesis of atropisomeric compounds with an N–C chiral axis. *Org. Prep. Proced. Int.* **46**, 1–23 (2014).
39. Ricci, A. *Amino Group Chemistry: from Synthesis to the Life Sciences* (Wiley–VCH, 2008).
40. Tsuji, N. et al. Activation of olefins via asymmetric Brønsted acid catalysis. *Science* **359**, 1501–1505 (2018).
41. Schreyer, L. et al. Confined acids catalyze asymmetric single aldolizations of acetaldehyde enolates. *Science* **362**, 216–219 (2018).
42. Akiyama, T., Itoh, J., Yokota, K. & Fuchibe, K. Enantioselective Mannich-type reaction catalyzed by a chiral Brønsted acid. *Angew. Chem. Int. Ed.* **43**, 1566–1568 (2004).
43. Uraguchi, D. & Terada, M. Chiral Brønsted acid-catalyzed direct Mannich reactions via electrophilic activation. *J. Am. Chem. Soc.* **126**, 5356–5357 (2004).
44. Zhuo, C.-X., Zhang, W. & You, S.-L. Catalytic asymmetric dearomatization reactions. *Angew. Chem. Int. Ed.* **51**, 12662–12686 (2012).
45. Gustafson, J., Lim, D. & Miller, S. J. Dynamic kinetic resolution of biaryl atropisomers via peptide-catalyzed asymmetric bromination. *Science* **328**, 1251–1255 (2010).
46. Barrett, K. T., Metrano, A. J., Rablen, P. R. & Miller, S. J. Spontaneous transfer of chirality in an atropisomerically enriched two-axis system. *Nature* **509**, 71–75 (2014).
47. Iorio, N. D. et al. Remote control of axial chirality: aminocatalytic desymmetrization of N-arylmaleimides via vinylogous Michael addition. *J. Am. Chem. Soc.* **136**, 10250–10253 (2014).
48. Zhang, J.-W. et al. Discovery and enantiocontrol of axially chiral urazoles via organocatalytic tyrosine click reaction. *Nat. Commun.* **7**, 10677 (2016).
49. Crawford, J. M., Stone, E. A., Metrano, A. J., Miller, S. J. & Sigman, M. S. Parameterization and analysis of peptide-based catalysts for the atroposelective bromination of 3-arylquinazolin-4(3*H*)-ones. *J. Am. Chem. Soc.* **140**, 868–871 (2018).
50. Li, T.-Z., Liu, S.-J., Tan, W. & Shi, F. Catalytic asymmetric construction of axially chiral indole-based frameworks: an emerging area. *Chem. Eur. J.* **26**, 15779–15792 (2020).
51. Frisch, M. J. et al. Gaussian 16, revision A.03 (Gaussian, 2016).
52. Chai, J. D. et al. Long-range corrected hybrid density functionals with damped atom-atom dispersion corrections. *Phys. Chem. Chem. Phys.* **10**, 6615–6620 (2008).
53. Cossi, M. et al. Energies, structures, and electronic properties of molecules in solution with the C-PCM solvation model. *J. Comput. Chem.* **24**, 669–681 (2003).
54. Luchini, G. et al. GoodVibes 3.0.1 10.5281/zenodo.595246 (2019).
55. Grimme, S. Supramolecular binding thermodynamics by dispersion-corrected density functional theory. *Chem. Eur. J.* **18**, 9955–9964 (2012).
56. Li, Y. et al. Improved force-field parameters for QM/MM simulations of the energies of adsorption for molecules in zeolites and a free rotor correction to the rigid rotor harmonic oscillator model for adsorption enthalpies. *J. Phys. Chem. C* **119**, 1840–1850 (2015).
57. Grimme, S. et al. Fully automated quantum-chemistry-based computation of spin-spincoupled nuclear magnetic resonance spectra. *Angew. Chem. Int. Ed.* **56**, 14763–14769 (2017).
58. Grimme, S. Exploration of chemical compound, conformer, and reaction space with metadynamics simulations based on tight-binding quantum chemical calculations. *J. Chem. Theory Comput.* **15**, 2847–2862 (2019).
59. Grimme, S. et al. A robust and accurate tight-binding quantum chemical method for structures, vibrational frequencies, and noncovalent interactions of large molecular systems parametrized for all spd-block elements ($Z = 1–86$). *J. Chem. Theory Comput.* **13**, 1989–2009 (2017).
60. Bannwarth, C. et al. GFN2-xTB—an accurate and broadly parametrized self-consistent tight-binding quantum chemical method with multipole electrostatics and density dependent dispersion contributions. *J. Chem. Theory Comput.* **15**, 1652–1671 (2019).
61. Pracht, P. et al. A robust non-self-consistent tight binding quantum chemistry method for large molecules. Preprint at *ChemRxiv* 10.26434/chemrxiv.8326202.v1 (2019).

Methods

Procedure for synthesis of N-aryl compounds (1–41)

In an oven-dried Schlenk tube, phosphoric acid **PA1** (10 mol%), **E-1** or **E-2** (0.20 mmol) and **N-1** or **N-2** (0.30 mmol) were dissolved in CH_2Cl_2 (0.05 M, 4 ml). The mixture was stirred at 25 °C until the reaction was completed (about 0.5 h). The solvent was removed under reduced pressure, and the residue was purified by column chromatography on silica gel (CH_2Cl_2/EtOAc = 50/1 as eluent) to give the pure product.

Procedure for CADA of 1-naphthols (42–54)

In an oven-dried Schlenk tube, (*R*)-**C5** (10 mol%), **E-1** (0.20 mmol) and **N-1** (0.30 mmol) were stirred at −40 °C for 5 min. Then, 4 ml toluene was added in one portion. After the completion of the reaction, the mixture was purified by preparative thin layer chromatography (TLC) (CH_2Cl_2/EtOAc = 50/1 as eluent) to give the pure product.

Procedure for atroposelective N-arylation (55–83)

In an oven-dried Schlenk tube, (*R*)-**C10** (7.5 mol%), **E-3** (0.20 mmol) and **N-2** (0.20 mmol) were dissolved in toluene (anhydrous, 0.05 M, 4 ml) under N_2. The mixture was stirred at 25 °C until the reaction was completed (about 4 h). The solvent was removed under reduced pressure, and the residue was purified by column chromatography on silica gel (CH_2Cl_2/PE = 2/1 as eluent) to give the pure product.

Procedure for atroposelective N-heteroarylation (84–114)

In an oven-dried Schlenk tube, (*R*)-**C12** (5 mol%), **E-4** (0.25 mmol) and **N-3** (0.20 mmol) were stirred under N_2 for 5 min. Then, anhydrous 1,2-dichlorethane (0.05 M, 4 ml) was added in one portion. The mixture was stirred at 25 °C until the reaction was completed (about 0.5 h). The solvent was removed under reduced pressure, and the residue was purified by preparative TLC (CH_2Cl_2 as eluent) to give the pure product.

Data availability

Crystallographic data for the structures reported in this article have been deposited at the Cambridge Crystallographic Data Centre (CCDC) under numbers CCDC 2181457 (**E-1a**), 2092420 (**1**), 2181572 (**27**), 2252804 (**45**), 2261521 (**49**), 2153493 (**73**), 1937417 (**84**) and 2252823 (**102**). Copies of the data can be obtained free of charge via https://www.ccdc.cam.ac.uk/structures/. The data supporting the findings of this work are provided in the Supplementary Information including experimental procedures and characterization of new compounds.

Acknowledgements

We are grateful for financial support from the National Natural Science Foundation of China (nos. 21825105 and 22231004 to B.T. and no. 22271135 to S.-H.X.), National Key R&D Program of China (nos. 2022YFA1503703 and 2021YFF0701604 to B.T.), National Science Foundation (CHE-1764328 to K.N.H.), Guangdong Innovative Program (no. 2019BT02Y335 to B.T.), Shenzhen Science and Technology Program (KQTD20210811090112004 and JCYJ20210324120205016 to B.T. and JCYJ20210324105005015 to S.-H.X.). Computational work was supported by the Center for Computational Science and Engineering at Southern University of Science and Technology, and the Extreme Science and Engineering Discovery Environment, which is supported by the National Science Foundation (OCI-1053575 to K.N.H.). The authors appreciate the assistance of SUSTech Core Research Facilities.

Author contributions

B.T. conceived and directed the project. Y.-H.C. designed and performed experiments. S.-L.L, Y.-W.L., J.K.C. and S.-H.X. helped with the collection of some new compounds and data analysis. M.D. and P.Y. performed the DFT calculations and mechanism analysis. K.N.H. directed the DFT calculations and mechanism analysis. B.T., Y.-H.C., M.D., J.K.C., S.-H.X. and K.N.H. wrote the paper with input from all other authors. All authors discussed the results and commented on the manuscript. Y.-H.C. and M.D. contributed equally to this work

Competing interests

The authors declare no competing interests.

Additional information

Supplementary information The online version contains supplementary material available at https://doi.org/10.1038/s41557-023-01384-x.

Correspondence and requests for materials should be addressed to Kendall N. Houk or Bin Tan.

Peer review information *Nature Chemistry* thanks the anonymous reviewers for their contribution to the peer review of this work.